Dielectric Relaxations due to the Interfacial Polarization in Bilamellar Structure

Theoretical Derivation in terms of Electrostatic Laws and the Consideration by Experiments

Kongshuang Zhao*, Kinzi Asaka**,
Katsuhisa Sekine** and Tetsuya Hanai**

On the basis of electrostatic laws, a dielectric theory is developed to explain dielectric relaxations due to the interfacial polarization in bilamellar structure composed of two phases. The derived formula is seen to be equivalent to that for a series combination of two lumped capacitance-conductance circuit models. Some dielectric observation is made on composite systems of drilled films and potassium chloride solutions, the results being in quantitative conformity with the dielectric theory proposed.

I. INTRODUCTION

Dielectric relaxations observed in heterogeneous materials are understood to be caused by the relaxation of interfacial polarization, the so-called Maxwell-Wagner relaxation[1-7]. The simplest system of such heterogeneous dielectrics is a series combination of two phases, each of which is represented routinely by a lumped capacitance-conductance $(C\text{-}G)$ model. This model, however, should be subjected to justification in terms of electrostatic field quantities and laws applied to the composite dielectrics prior to the use of a lumped $C\text{-}G$ model.

In the present work, a heterogeneous dielectric in bilamellar structure is formulated theoretically by means of electrostatic laws to show the dielectric relaxations. In view of the derived relation, the bilamellar structure is seen to be equivalent to a series combination of the lumped $C\text{-}G$ models. Some experimental results of dielectric relaxation observed in the bilamellar dielectrics are shown to confirm the theoretical formulation.

II. THEORETICAL

2.1 Fundamental Relations in the Quasi-electrostatic Field

A diphase system in bilamellar structures is depicted in Fig. 1, which is com-

---

* 趙 孔双 : Department of Chemistry, Northeast Normal University, Changchun, China.
** 安積欣志, 関根克尚, 花井哲也 : Laboratory of Dielectrics, Institute for Chemical Research, Kyoto University, Uji, Kyoto 611. Japan.

charge density σ

electrode   on the boundary   electrode

b   a

Phase b   **Phase a**

electrode   electric field $\vec{E_b}$ $\vec{E_a}$

charge Q_b el. flux density $\vec{D_b}$ $\vec{D_a}$ Q_a

distance |———— d_b ————→|—— d_a ——|

               |————— whole, d ————→|

permittivity ε_b ε_a

conductivity κ_b κ_a

$$E_b = \frac{D_b}{\varepsilon_v \varepsilon_b} \qquad E_a = \frac{D_a}{\varepsilon_v \varepsilon_a}$$

potential difference |←——— V_b ———|←—— V_a ——|

$$V_b = E_b d_b \qquad V_a = E_a d_a$$

$V = V_b + V_a$ |←——— whole, V ———|

current $\vec{i_b} = \kappa_b E_b$ $\vec{i_a} = \kappa_a E_a$

increasing rate of σ $\dfrac{d\sigma}{dt} = i_b - i_a$

Q_b → i_b i_a→ Q_a

I   I

          by external V–source

$$I = \frac{dQ_b}{dt} + i_b \qquad\qquad I = -\frac{dQ_a}{dt} + i_a$$

flux density D

D due to Q_b ——→ $Q_b/2$ ——→ $Q_b/2$

D due to Q_a ←— $-Q_a/2$ ←— $-Q_a/2$

D due to σ ←— $-\sigma/2$ ——→ $\sigma/2$

total D $D_b = \dfrac{Q_b}{2} - \dfrac{Q_a}{2} - \dfrac{\sigma}{2}$ $D_a = \dfrac{Q_b}{2} - \dfrac{Q_a}{2} + \dfrac{\sigma}{2}$
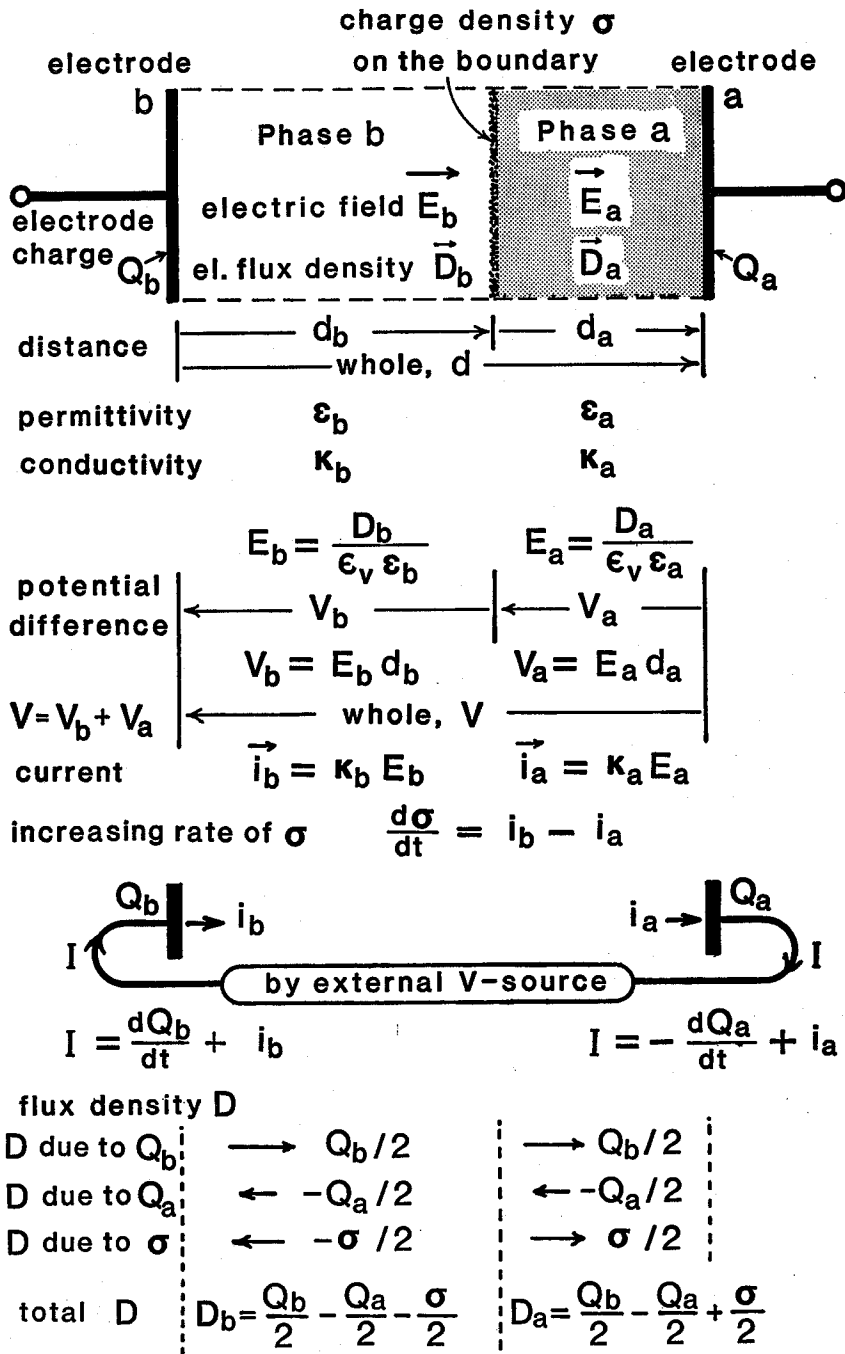
Fig. 1. Quasi-electrostatic fields, the related electric phenomena and the laws concerned for a bilamellar structure in a parallel-plate capacitor.

posed of Phase b (henceforth referred to with a subscript b) and phase a (subscript a) inserted in a parallel-plate capacitor with unit area. Each electrode plate is charged with the electric charge Q_b or Q_a respectively. The charge density σ is assumed to accumulate on the boundary between Phases b and a. Figure 1 includes electrostatic laws and expressions necessary for the explanation below, where vector quantities are assumed to have positive values for pointing to the right.

The electrode charges Q_b, Q_a and the boundary charge density σ in planar distribution give rise to the constituent parts of the electric flux density as shown in the lowest part of Fig. 1, the electric flux densities D_b and D_a being represented as the following:

$$D_b = \frac{Q_b - Q_a}{2} - \frac{\sigma}{2} , \tag{1}$$

$$D_a = \frac{Q_b - Q_a}{2} + \frac{\sigma}{2} . \tag{2}$$

The relation between the flux density D_b or D_a and the electric field E_b or E_a is given by

$$E_b = \frac{D_b}{\epsilon_V \epsilon_b} , \quad \text{and} \quad E_a = \frac{D_a}{\epsilon_V \epsilon_a} , \tag{3}$$

respectively, where ϵ is the relative permittivity of the respective phase, and ϵ_V is the permittivity of vacuum.

Potential differences V_b and V_a for respective phases are given by

$$V_b = E_b d_b , \quad \text{and} \quad V_a = E_a d_a , \tag{4}$$

where d_b or d_a denotes the thickness of the respective phases. The total potential difference V is the sum of V_b and V_a, that is,

$$V = V_b + V_a . \tag{5}$$

Using the electrical conductivities κ_b and κ_a, the electric current i_a and i_b are given by

$$i_b = \kappa_b E_b , \quad \text{and} \quad i_a = \kappa_a E_a . \tag{6}$$

As regards the charge density σ per unit area on the boundary surface between Phase b and Phase a, its increasing rate against time t is the difference of the current i_b and i_a, that is,

$$\frac{d\sigma}{dt} = i_b - i_a . \tag{7}$$

The inflow current I must be equal to the outflow current owing to the total charge conservation law, being given by

$$\frac{dQ_b}{dt} + i_b = I = -\frac{dQ_a}{dt} + i_a . \tag{8}$$

From Eqs. 8 and 7, we have

$$\frac{d}{dt}(Q_b + Q_a) = -i_b + i_a = -\frac{d\sigma}{dt} . \tag{9}$$

Integrating Eq. 9 with null integration constant corresponding the neutral condition, we have

$$Q_b + Q_a = -\sigma . \tag{10}$$

For simplicity, we put as follows:

$$\delta_b \equiv \frac{d_b}{\epsilon_V \varepsilon_b} = \frac{1}{C_b} \ , \quad \delta_a \equiv \frac{d_a}{\epsilon_V \varepsilon_a} = \frac{1}{C_a} \ , \tag{11}$$

$$k_b \equiv \frac{\kappa_b}{\epsilon_V \varepsilon_b} = \frac{G_b}{C_b} \ , \quad k_a \equiv \frac{\kappa_a}{\epsilon_V \varepsilon_a} = \frac{G_a}{C_a} \ , \tag{12}$$

where C_b, G_b, C_a and G_a are the lumped capacitance and the lumped conductance of Phases b and a respectively, the details being discussed in a later section concerning a lumped impedance model.

2.2 Solution in AC Field and the Derivation of the Electrical Quantities

By use of Eqs. 5, 3, 4 and 11, we have

$$V = D_b \delta_b + D_a \delta_a \ . \tag{13}$$

Substituting Eqs. 1, 2 and 11 into Eq. 13, we have

$$V = \frac{1}{2} (\delta_b + \delta_a)(Q_b - Q_a) - \frac{1}{2}(\delta_b - \delta_a)\sigma \ . \tag{14}$$

Thus Eq. 14 can be rearranged to an explicit form with respect to $(Q_b - Q_a)$:

$$Q_b - Q_a = \frac{\delta_b - \delta_a}{\delta_b + \delta_a}\sigma + \frac{2}{\delta_b + \delta_a}V \ . \tag{15}$$

Substituting Eqs. 6, 3, 2 and 12 into Eq. 7, we have

$$\frac{d\sigma}{dt} = \frac{1}{2}(k_b - k_a)(Q_b - Q_a) - \frac{1}{2}(k_b + k_a)\sigma \ . \tag{16}$$

Substituting Eq. 15 into Eq. 16 to eliminate $(Q_b - Q_a)$, we have

$$\frac{d\sigma}{dt} = -\frac{k_b \delta_a + k_a \delta_b}{\delta_b + \delta_a}\sigma + \frac{k_b - k_a}{\delta_b + \delta_a}V \ . \tag{17}$$

Equation 17 is a linear differential equation of first-order with respect to time t, where V is assumed to be ac voltage supplied by an external generator. A stationary state solution of Eq. 17 under ac voltage with a frequency ω can be written in the following form:

$$\sigma = \frac{k_b - k_a}{k_b \delta_a + k_a \delta_b} \cdot \frac{1}{1 + j\dfrac{\omega}{\omega_0}}V \ , \tag{18}$$

with

$$\omega_0 \equiv \frac{k_b \delta_a + k_a \delta_b}{\delta_b + \delta_a} \ , \tag{19}$$

where ω_0 is the relaxation frequency characterizing the dielectric relaxation, and j is the imaginary unit.

From Eqs. 10 and 15, we obtain

$$Q_b = -\frac{\delta_a}{\delta_b + \delta_a}\sigma + \frac{1}{\delta_b + \delta_a}V \ , \tag{20}$$

and

$$Q_a = -\frac{\delta_b}{\delta_b + \delta_a}\sigma - \frac{1}{\delta_b + \delta_a}V \ . \tag{21}$$

Substituting Eqs. 3, 1, 2 and 15 into Eq. 6, we can derive

$$i_b = \frac{k_b}{\delta_b + \delta_a}(-\delta_a \sigma + V) \ , \tag{22}$$

and

$$i_a = \frac{k_a}{\delta_b + \delta_a}(\delta_b \sigma + V) \ . \tag{23}$$

2.3 Derivation of the Permittivity Formula for the Whole System

The relation between the current I for the capacitor system and the total potential difference V shown in Fig. 1 can be written as

$$I = j\omega\left(\frac{\varepsilon^*\epsilon_V}{d}\right)V ,\tag{24}$$

where d is the total thickness of the capacitor, and ε^* is the complex relative permittivity of the whole system. From Eqs. 24 and 8, we have

$$\varepsilon^* = d\frac{I}{j\omega\epsilon_V V} = d\frac{j\omega Q_b + i_b}{j\omega\epsilon_V V} .\tag{25}$$

Equations 20, 22 and 18 are substituted into Eq. 25 to eliminate Q_b and i_b. After somewhat cumbersome calculation with the aid of the general formula

$$\frac{1}{j\omega\left(1+j\dfrac{\omega}{\omega_0}\right)} = \frac{1}{j\omega} + \frac{-\dfrac{1}{\omega_0}}{1+j\dfrac{\omega}{\omega_0}} ,\tag{26}$$

the following formula can be derived:

$$\varepsilon^* = d\frac{1}{\epsilon_V(\delta_b+\delta_a)} + d\frac{\delta_b\delta_a(k_b-k_a)^2}{\epsilon_V(\delta_b+\delta_a)(k_b\delta_a+k_a\delta_b)^2}\cdot\frac{1}{1+j\dfrac{\omega}{\omega_0}}$$
$$+ d\frac{1}{j\omega\epsilon_V}\cdot\frac{k_b k_a}{k_b\delta_a+k_a\delta_b} .\tag{27}$$

Equations 27 and 19 are rearranged as

$$\frac{\varepsilon^*}{d} = \frac{1}{\dfrac{d_b}{\varepsilon_b}+\dfrac{d_a}{\varepsilon_a}} + \frac{\dfrac{d_b}{\varepsilon_b}\dfrac{d_a}{\varepsilon_a}\left(\dfrac{\kappa_b}{\varepsilon_b}-\dfrac{\kappa_a}{\varepsilon_a}\right)^2}{\left(\dfrac{d_b}{\varepsilon_b}+\dfrac{d_a}{\varepsilon_a}\right)\left(\dfrac{\kappa_b}{\varepsilon_b}\dfrac{d_a}{\varepsilon_a}+\dfrac{\kappa_a}{\varepsilon_a}\dfrac{d_b}{\varepsilon_b}\right)^2}\cdot\frac{1}{1+j\dfrac{\omega}{\omega_0}}$$
$$+ \frac{1}{j\omega\epsilon_V}\cdot\frac{\dfrac{\kappa_b}{\varepsilon_b}\dfrac{\kappa_a}{\varepsilon_a}}{\dfrac{\kappa_b}{\varepsilon_b}\dfrac{d_a}{\varepsilon_a}+\dfrac{\kappa_a}{\varepsilon_a}\dfrac{d_b}{\varepsilon_b}} ,\tag{28}$$

and

$$\omega_0 = \frac{1}{\epsilon_V}\cdot\frac{\dfrac{\kappa_b}{\varepsilon_b}\dfrac{d_a}{\varepsilon_a}+\dfrac{\kappa_a}{\varepsilon_a}\dfrac{d_b}{\varepsilon_b}}{\dfrac{d_b}{\varepsilon_b}+\dfrac{d_a}{\varepsilon_a}} .\tag{29}$$

Recently Bánhegyi[8] derived formulas of dielectric relaxations of bilayer dielectrics composed of relaxing components. The formulas are rather complicated to provide us with an overall view of the relaxation characteristics. His analytical formulas are simplified to Eqs. 28 and 29 by adopting non-relaxing components, though the paper is lacking in simplified expressions.

2.4 Relation to the Lumped C-G Model

By use of Eqs. 11 and 12, Eqs. 28 and 29 are transformed to the following formula which is represented in terms of the quantities C_b, C_a, G_b and G_a of the lumped C-G model:

$$C^* = \frac{C_b C_a}{C_b+C_a} + \frac{(G_b C_a - G_a C_b)^2}{(C_b+C_a)(G_b+G_a)^2}\cdot\frac{1}{1+j\dfrac{\omega}{\omega_0}} + \frac{1}{j\omega}\cdot\frac{G_b G_a}{G_b+G_a} ,\tag{30}$$

and

$$\omega_0 = \frac{G_b + G_a}{C_b + C_a} .$$
(31)

A homogeneous and conductive dielectric, termed Phase a, characterized by the permittivity ε_a and the conductivity κ_a is represented routinely by a parallel-combination model of a lumped capacitance C_a and a lumped conductance G_a. From the viewpoint of circuit model, a bilamellar structure composed of such Phases a and b shown in Fig. 1 is represented by a series combination of the parallel equivalent C_a-G_a and the parallel equivalent C_b-G_b as depicted in Fig. 2.
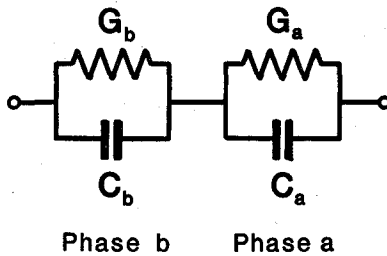
Fig. 2. A circuit model to simulate the bila-
mellar structure which is illustrated
in Fig. 1. G_b and C_b: lumped
parallel-equivalent conductance and
capacitance of Phase b. G_a and C_a:
lumped parallel-equivalent conduc-
tance and capacitance of Phase a.
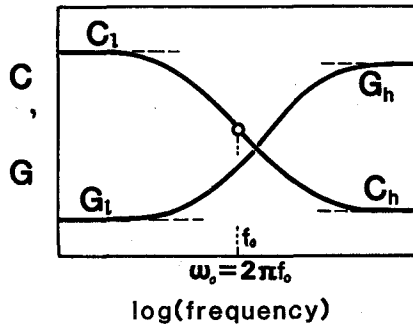
Fig. 3. Frequency dependence of the capaci-
tance C and the conductance G of a
circuit model shown in Fig. 2.

After some impedance calculation for the circuit model of Fig. 2, it turns out that the frequency dependence of the capacitance and the conductance of the whole system is given by equations just the same as Eqs. 30 and 31, the profile of frequency dependence being shown in Fig. 3.   It is thus verified theoretically that the bilamellar structure under quasi-electrostatic field shown in Fig. 1 can be simulated by the circuit model depicted in Fig. 2 and the associated Eqs. 30 and 31.

III.   TREATMENT OF OBSERVED DATA IN CONNECTION WITH EVALUATION OF PHASE PARAMETERS ε AND κ

In practice of dielectric measurements, an overall profile is observed of the frequency dependence of the capacitance C and the conductance G of specimens to determine the limiting values C_l, C_h, G_l and G_h at low (subscript l) and high (h) frequencies.

As the limiting cases of Eq. 30 at low and at high frequencies, the expressions of C_h, C_l, G_h and G_l can readily be derived from Eq. 30 as the following:

$$C_h = \frac{C_b C_a}{C_b + C_a} ,$$
(32)

$$C_l = \frac{C_b G_a^2 + C_a G_b^2}{(G_b + G_a)^2} ,$$
(33)

$$G_h = \frac{G_b C_a{}^2 + G_a C_b{}^2}{(C_b + C_a)^2} , \tag{34}$$

$$G_l = \frac{G_b G_a}{G_b + G_a} . \tag{35}$$

The phase parameters C_b, C_a, G_b and G_a are thus represented by C_l, C_h, G_l and G_h as follows[9]:

$$A = \left[\left(1 - \frac{G_l}{G_h} \right)^{-1} - \left(\frac{C_l}{C_h} - 1 \right)^{-1} \right] \left(\frac{C_l}{C_h} - 1 \right)^{1/2} , \tag{36}$$

$$Y_a = \frac{1}{2} - \frac{1}{2} \left[1 + \left(\frac{2}{A} \right)^2 \right]^{-1/2} , \tag{37}$$

$$C_a = \frac{C_h}{Y_a} , \tag{38}$$

$$C_b = \frac{C_h}{1 - Y_a} , \tag{39}$$

$$X_a = Y_a + \left[Y_a (1 - Y_a) \left(\frac{C_l}{C_h} - 1 \right) \right]^{1/2} \quad \text{for} \quad A > 0 , \tag{40}$$

$$X_a = Y_a - \left[Y_a (1 - Y_a) \left(\frac{C_l}{C_h} - 1 \right) \right]^{1/2} \quad \text{for} \quad A < 0 , \tag{41}$$

$$G_a = \frac{G_l}{X_a} , \tag{42}$$

$$G_b = \frac{G_l}{1 - X_a} , \tag{43}$$

$$\omega_0 = 2\pi f_0 = \frac{G_h - G_l}{C_l - C_h} . \tag{44}$$

Next, ε_b, ε_a, κ_b and κ_a can be calculated by use of Eqs. 11 and 12 provided that d_b and d_a are known.

IV. DIELECTRIC OBSERVATIONS OF DRILLED FILMS IMMERSED IN AQUEOUS SOLUTIONS AS VIEWED FROM THE THEORY FOR THE BILAMELLAR STRUCTURE

With a view to examining the theory discussed above, dielectric measurements were carried out for systems composed of drilled Teflon films and KCl aqueous solutions by use of a measuring cell shown in Fig. 4.

Capacitance C and conductance G of this composite system were measured with a Model 4192A LF Impedance Analyser made by Hewlett-Packard Co., Ltd. over a frequency range from 5 Hz to 13 MHz at 25°C.

The Teflon films of 0.095 mm in thickness are drilled by 0, 8, 16 or 25 holes of about 0.3 mm in diameter. Dielectric measurements were carried out for the systems of respective films immersed in KCl solutions of different concentrations.

4.1 Observation of Dielectric Relaxations for the Film-Solution Systems

The observed results for a film with 25 holes (abbreviated to 25 hole-film) are shown in Fig. 5, the complex capacitance plane plots being shown in Fig. 6. Distinct dielectric relaxations are found in a frequency range of 10^4 to 10^6 Hz, being assumed to be those given by Eq. 30. The relaxation frequency f_0 shifts to higher frequencies in proportion to KCl concentration in the aqueous phases as shown in Fig. 7. The values of C_l, C_h, G_l, G_h and f_0 are obtained from Figs. 5 and 6.

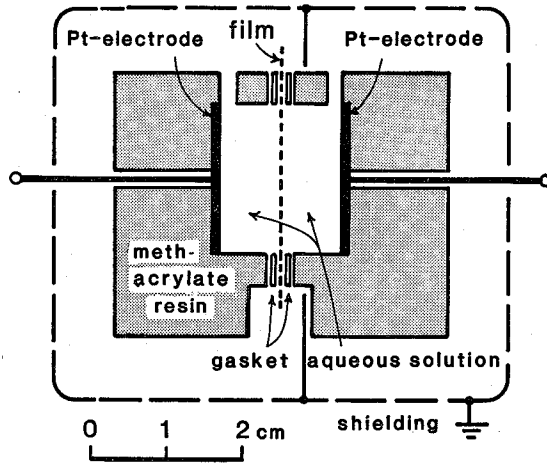Dielectric Relaxation in Bilamellar Structure

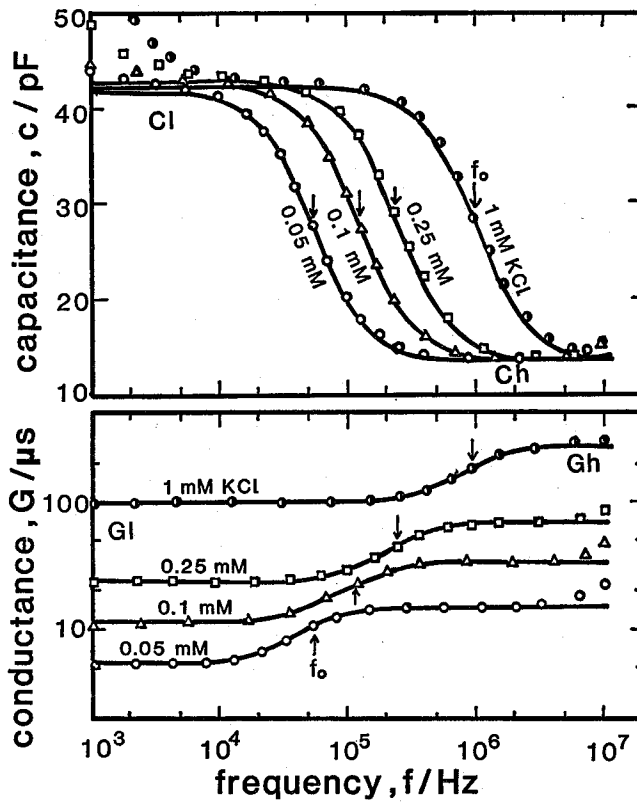Fig. 4. Cell system for measuring the impedance of a
film-solution system.

Fig. 5. Frequency dependence of the capacitance C and the
conductance G for systems of a 25 hole-film immersed
in KCl solutions of 0.05, 0.1, 0.25 and 1 mM. Solid
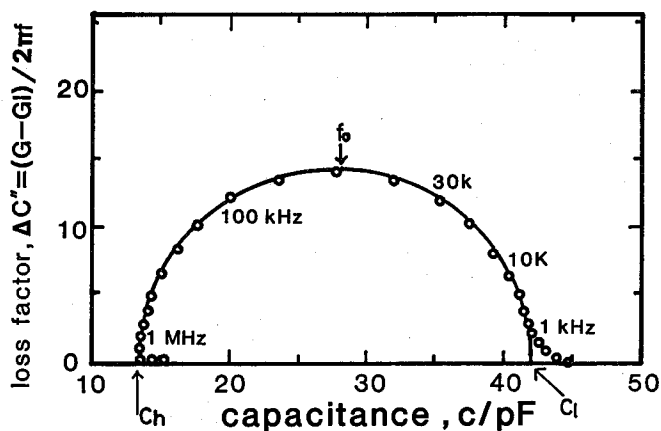curves are calculated by use of Eqs. 30 and 31.

(547)

Fig. 6. Complex plane plots of the complex capacitance $C^*=C-j\Delta C''$ for a system of a 25 hole-film immersed in a 0.05 mM KCl solution. The data referring to Fig. 5.
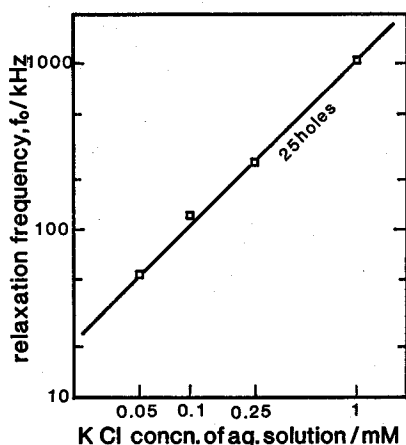

Fig. 7. Dependence of the relaxation frequency f_0 upon the KCl concentration of the aqueous solution for systems including a 25 hole-film.

Values of C_a, G_a, C_b, G_b and f_0 are also calculated from these values of C_l, C_h, G_l and G_h by use of Eqs. 36 to 44. Values of ε_a, κ_a, ε_b and κ_b are calculated by use of Eqs. 11 and 12 provided d_b and d_a are measured directly. The part of these data are listed in Table I. The value of ε_a for no holes is very close to that of the film material (Teflon, $\varepsilon_T=2.08-2.1$[10]). The values of ε_b for the aqueous phases are in good agreement with that of water (water at 25°C, $\varepsilon_W=78.30$[11]). Observed data for the systems of the films with 0, 8, 16 or 25 holes immersed in 1 mM KCl solutions are shown partly in Figs. 8 and 9. Solid curves in Figs. 5 to 9 are calculated from the values of C_a, C_b, G_a and G_b in Table I by use of Eqs. 30 and 31, being in good agreement with the observed values.

The following are thus confirmed by the electrostatic field laws and the exper-

Table I. Dielectric Parameters Observed and Phase Parameters Calculated for the Cell Systems Composed of drilled Teflon films and the Ambient KCl Solutions at 25°C

Number of holes	Dielectric parameters observed						Phase parameters calculated									
	$\frac{\text{KCl}}{\text{mM}}$	$\frac{C_l}{\text{pF}}$	$\frac{C_h}{\text{pF}}$	$\frac{G_l}{\mu\text{S}}$	$\frac{G_h}{\mu\text{S}}$	$\frac{f_0}{\text{kHz}}$	$\frac{C_a}{\text{pF}}$	$\frac{G_a}{\mu\text{S}}$	$\frac{C_b}{\text{pF}}$	$\frac{G_b}{\mu\text{S}}$	$\frac{f_0}{\text{kHz}}$	$\frac{G_a}{G_b}$ [a]	ε_a	ε_b	$\frac{\kappa_a}{\text{nS cm}^{-1}}$	$\frac{\kappa_b}{\mu\text{S cm}^{-1}}$ [b]
16	0.05	46.8	13.0	3.57	14.6	52	65.7	4.25	16.3	22.4	52	0.190	2.17	78.2	12.6	9.54
16	0.1	46.4	13.1	8.06	32.6	117	65.2	9.59	16.4	50.5	117	0.190	2.18	78.9	28.4	21.5
16	0.25	47.1	13.1	17.07	68.4	244	66.5	20.4	16.4	104.9	241	0.194	2.22	78.7	60.3	44.7
16	1.0	48.2	13.2	68.9	273	968	68.8	82.7	16.4	413	927	0.200	2.30	78.6	245	176
0	0.25	62.2	13.0	0.0	65.6	215	62.2	0.0	16.5	104.2	212	0.0	2.08	79.3	0.0	44.4
8	0.25	54.5	13.1	8.87	68.6	231	64.6	9.67	16.4	107.2	230	0.0902	2.16	78.9	28.6	45.7
25	0.25	43.0	13.3	23.3	69.0	252	69.7	30.0	16.5	103.8	247	0.289	2.33	79.3	88.7	44.2

Film thickness, d_a =0.095 mm; Film area, S=3.14 cm^2; Hole diameter=about 0.3 mm.

a) Calculated from the observed C_l, C_h, G_l and G_h by use of Eqs. 36 to 44.

b) Calculated from the calculated C_a, C_b, G_a and G_b by use of Eqs. 11 and 12, where d_b=1.30 cm and ϵ_V=0.088541 pF cm^{-1}.
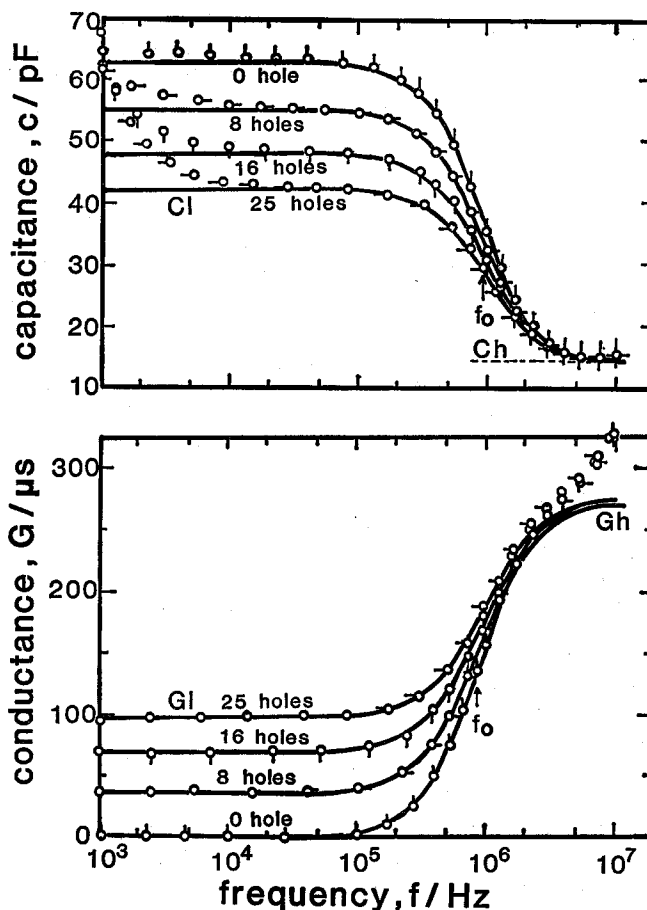
Fig. 8. Frequency dependence of the capacitance C and the conductance G for systems of 0, 8. 16 and 25 hole-films immersed in 1 mM KCl solutions. Solid curves are calculated by use of Eqs. 30 and 31.

iment:

(i) From the viewpoint of the electrostatic field analysis, it is justified that the lumped capacitance-conductance model is valid for the lamellar structure.

(ii) The permittivity and the conductivity of the constituent phases in lamellar structure can be evaluated in reason by use of Eqs. 11 and 12.

4.2 Further Consideration on C_a, C_b, G_a and G_b obtained for the Films

Closer inspection of Table I revealed the following feature of observations on the drilled films immersed in aqueous solutions.

The capacitance C_b of the aqueous phase shows definite values irrespective of both the KCl concentration and the number of holes. The conductance G_b and κ_b of the aqueous phase vary in proportion to the KCl concentration of the aqueous phase irrespective of the number of holes on the films as seen in Table I and Fig. 10.
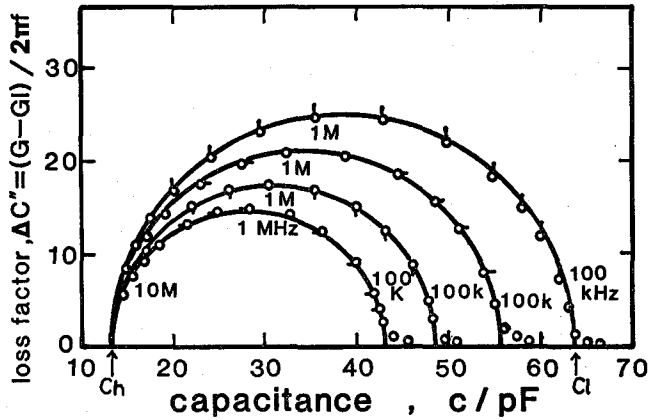
(550)

Fig. 9. Complex plane plots of the complex capacitance $C^*=C-j\Delta C''$ for systems of drilled films immersed in 1 mM KCl solutions. The data referring to Fig. 8.
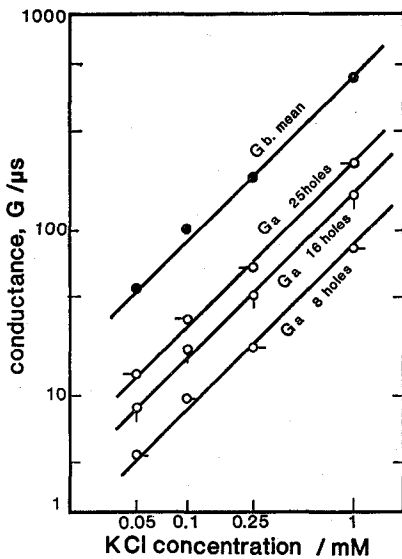

Fig. 10. KCl concentration dependence of conductances G_b and G_a which are calculated from the observed values of C_l, C_h, G_l and G_h by using Eqs. 36 to 43. G_b: conductance of the KCl solutions as an average over the films with 0, 8, 16 and 25 holes. G_a: conductance of the drilled films.
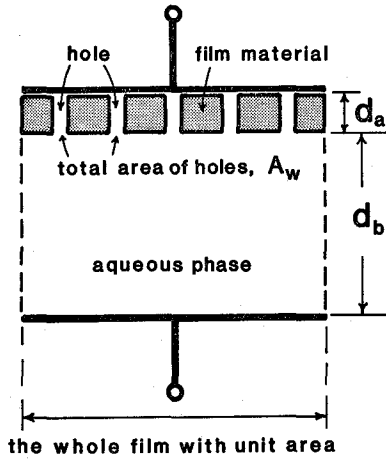
Fig. 11. Schematic cross section of a drilled film and the ambient aqueous phase in series combination.

The capacitance C_a and ε_a of the drilled films are dependent upon the number of holes, being independent of the KCl concentration of the aqueous phase. The conductance G_a and κ_a of the films are dependent upon both the number of holes and the KCl concentration of the aqueous phase. It is worth while noting that a ratio G_a/G_b shows values independent of the KCl concentration and depen-

dent on the number of holes. This feature means that the film conductance G_a is caused by the holes filled with the ambient KCl solution. Since it is difficult to measure accurately the total area of the holes in the respective films, the following analysis is put forward to elucidate the correlation between C_a and G_a.

As depicted in Fig. 11, a Teflon film with unit area is assumed to have some holes, whose area-fraction to total area of the film is A_W. When the holes are all filled with the ambient KCl solution, the capacitance C_a for the whole film is given by

$$C_a = \varepsilon_T \epsilon_V \frac{1-A_W}{d_a} + \varepsilon_W \epsilon_V \frac{A_W}{d_a} ,$$ (45)

where ε_T and ε_W are the permittivity of Teflon and water respectively. On the other hand, the film capacitance $C_{a,0}$ for no holes and the aqueous phase capacitance C_b are given by

$$C_{a,0} = \varepsilon_T \epsilon_V \frac{1}{d_a} , \quad \text{and} \quad C_b = \varepsilon_W \epsilon_V \frac{1}{d_b} ,$$ (46)

respectively. The conductance ratio G_a/G_b is given by

$$\frac{G_a}{G_b} = \frac{d_b A_W}{d_a} .$$ (47)

Substituting Eqs. 46 and 47 for Eq. 45, we have

$$\frac{C_a - C_{a,0}}{C_b} = \left(1 - \frac{\varepsilon_T}{\varepsilon_W}\right) \cdot \frac{G_a}{G_b} .$$ (48)
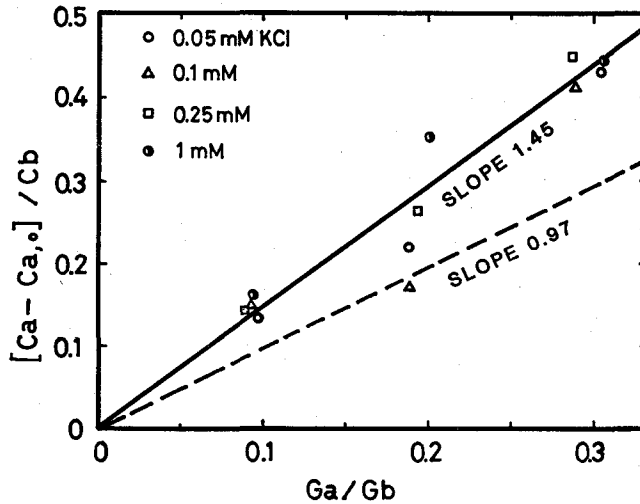

Fig. 12. Correlation between C_a and G_a for the respective films. The slope of a $(C_a - C_{a,0})/C_b$ vs. G_a/G_b diagram is 1.45 for the observed data, being 0.973 from the theory.

Figure 12 shows the plots of $(C_a - C_{a,0})/C_b$ against G_a/G_b for the observed data shown above. The plots are somewhat scattered around a straight line with a slope 1.45. By use of values $\varepsilon_T = 2.1$ for Teflon and $\varepsilon_W = 78.30$ for water, the slope predictable from Eq. 48 is evaluated as $(1 - \varepsilon_T/\varepsilon_W) = 0.973$, which is lower than the observed values.

For making this discrepancy clear, it is necessary to improve the measuring accuracy by drilling larger and clearer holes in the Teflon films. From the viewpoint of a model system for lossy films, these mechanically drilled films should be investigated further apart from the discussion of the present theory.

REFERENCES

(1) L.K.H. van Beek, Dielectric Behavior of Heterogeneous Systems in "Progress in Dielectric", Vol. 7, edited by J.B. Birks, Heywood Books, London. pp. 69–114 (1967).

(2) T. Hanai, Electrical Properties of Emulsions in "Emulsion Science", Chap. 5, edited by P. Sherman, Academic Press, London-New York. pp. 353–478 (1968).

(3) S.S. Dukhin, Dielectric Properties of Disperse Systems in "Surface and Colloid Science", Vol. 3, edited by Egon Matijevic, Wiley-Interscience, New York-London. pp. 83–165 (1971).

(4) S.S. Dukhin and V.N. Shilov, Dielectric Phenomena and the Double Layer in Disperse Systems and Polyelectrolytes, John Wiley and Sons, New York-Toronto-Jerusalem (1974).

(5) H.P. Schwan, Electrical Properties of Tissue and Cell Suspensions in "Advances in Biological and Medical Physics", Vol. 5, edited by J.H. Lawrence and C.T. Tobias, Academic Press, New York and London. pp. 147–209 (1957).

(6) R. Pething, Interfacial Dielectric Phenomena in Biological Systems in "Dielectric and Electronic Properties of Biological Materials", Chap. 5, John Wiley and Sons, New York. p. 150 (1979).

(7) M. Clausse, Dielectric Properties of Emulsions and Related Systems in "Encyclopedia of Emulsion Technology", Vol. 1, edited by P. Becher, Marcel Dekker Inc., New York and Basel. pp. 481–715 (1983).

(8) G. Bánhegyi, *Colloid and Polymer Sci.,* **262**, 956 (1984).

(9) H.Z. Zhang, T. Hanai and N. Koizumi, *Bull. Inst. Chem. Res., Kyoto Univ.,* **61**, 265 (1983).

(10) A.R. von Hippel, editor, Dielectric Materials and Applications, the Technology Press M.I.T. and John Wiley & Sons, Inc., New York. p. 332 (1954).

(11) C.G. Malmberg and A.A. Maryott, *J. Res. Nat. Bur. Standards,* **56**, 1 (1956).